Figure 4. *a*. Potted plants of *R. tetraphylla*: *b*, Potted plants of *R. micrantha*.

in vitro flowering which we observed in 20–40% of these cultures (Figure 2 *a* and *b*).

From proliferated shoot clumps, individual shoots were rooted within two weeks (Figure 3 *a* and *b*) and Table 2 indicates the rooting response in the two species. Roots produced in auxin-free media were thin and the number of roots/cutting were low. Media supplemented with IBA, 2 mg/l improved rooting frequency by 7–8% in both the species. Doubling sucrose in the rooting medium increased the percentage of rooting by 26% in *R. tetraphylla* and 20% in *R. micrantha*. A mortality of 43% was observed during *ex-vitro* rooting. After four weeks the plants were transplanted into pots (Figure 4 *a* and *b*). Plants taken from auxin-supplemented media survived transfer to soil better than those taken from auxin-free media.

The induction of multiple shoots through axillary branching is now recognized as a useful technique for propagation. The present work demonstrates a simple procedure for rapid clonal multiplication of *Rauvolfia* species through axillary branching. The number of shoots formed was best when BA was amended with low adenine sulphate levels. Individual plants may be accli-

matized by rooting the shoots *ex vitro*. Thus by this technique, *in vitro* conservation of threatened plants, especially those in which roots contain the active compound[14], is possible.

1. Nayar, M. P. and Sastry, A. R. K., *Red Data Book of Indian Plants*, Botanical Survey of India, Calcutta, 1987, vol. I.
2. Anonymous, in *The Wealth of India, Raw Materials*, Publications and Information Directorate, CSIR, New Delhi, 1969, vol. VIII.
3. Gupta, R., *Indian J. Plant Genet. Res.*, 1989, 1, 98–102.
4. Gamble, J. S., *Flora of Madras Presidency*, 1921, vol. 2, p. 808.
5. Henry, A. N., Kumari, G. R. and Chithra, V., *Flora of Tamil Nadu, India*, Botanical Survey of India Calcutta, 1987, vol. 2, p. 79.
6. Roja, P. C., Sipahimalani, A. T., Heble, M. R. and Chadha, M. S., *J. Nat. Products*, 1987, 50, 872–875.
7. Ilahi, I., Akram, M. and Kruas, L., *Pak. J. Sci. Ind. Res.*, 1988, 31, 114–117.
8. Mathur, A., Mathur, A. K., Kukreja, A. K., Ahuja, P. S., Tyagi, B. R. and Mathur, A., *Plant Cell Tiss. Organ Cult.*, 1987, 10, 129–134.
9. Ilahi, I. and Akram, A., *Pak. J. Agric. Res.*, 1987, 8, 204–210.
10. Upadhyay, N., Makoveychuk, A. Y., Nikolaeva, L. A. and Batygina, T. B., *J. Plant Physiol.*, 1992, 140, 218–222.
11. Murashige, T. and Skoog, F., *Physiol. Plant.*, 1962, 15, 473–497.
12. Sudha, C. G. and Seeni, S., *Plant Cell Rep.*, 1996, 44, 243–248.
13. George, E. F. and Sherrington, P. D., *Plant Propagation by Tissue Culture*, Exgenetics Limited, 1984, p. 243.
14. Sharma, N. and Chandel, K. P. S., *Plant Cell Rep.*, 1992, 11, 200–203.

Quaternary radiolarian faunal changes in the tropical Indian Ocean: Inferences to paleomonsoonal oscillation of the 10°S hydrographic front

Shyam M. Gupta and A. A. Fernandes
National Institute of Oceanography, Goa 403 004, India

The northern Indian Ocean is characterized by three distinct surface water masses, i.e. (i) highly saline (> 34.5 ppt) Arabian Sea, (ii) low saline (< 34.5 ppt) Bay of Bengal and (iii) a moderate salinity Indian Ocean watermass south of 10°S hydrographic front. Hence, changes in the surface salinity in this region are index for the paleomonsoon. Radiolaria, the oceanic microplanktons, are extremely sensitive to the

monsoonal salinity, temperature and productivity in the tropical Indian ocean. We refined the earlier radiolarian factor assemblage model by relinquishing the rare groups (< 2% abundance) that caused noise and suppressed the environmental signals. Refined analysis resulted in an additional factor characterizing the 10°S hydrographic front. The 4-factor based radiolarian model exhibited better relationship with the surface hydrographic characteristics of the overlying watermasses. We studied changes in down-core factor values in a sediment core SK-69/1, which has an excellent geological record for the last 0.2–1.4 million years. Down-core factorial fluctuations corroborate to changes in the paleomonsoon. Conspicuous variation in the values of factor-4 (0.2–0.6) characterized the oscillation of 10°S hydrographic front due to changes in the regional oceanic precipitation over the core-site coupled with variations in the monsoonal fresh water debauched by the Indian rivers into the Bay of Bengal. The frontal oscillation indicated an apparent cyclicity of ~ 120,000 years (± 20,000), which corresponds to the ~100,000 years Earth's orbital eccentricity cycle during the Quaternary.

THE Asian monsoonal rainfall is the backbone of the Indian subcontinent and the southeast Asian countries. The paleomonsoonal study may provide information on the behaviour of monsoon in the geological past which may be used for the monsoonal modelling. The present study attempts to record the monsoonal changes in the tropical Indian Ocean using proxy data of radiolarian microplanktons. Although the monsoon is an atmospheric phenomenon, it has a pronounced effect on the surface salinity due to enormous freshwater flux $(90 \times 10^3 \text{ m}^3/\text{s})$ through the Ganges–Bramhaputra rivers during July–August (peak of SW monsoon) into the Bay of Bengal[1]. However, it is a very conservative estimate because several other rivers [Krishna, Cauvery, Mahanandi, Godavari and Irrawadi (Myanmar)] also discharge huge amounts of freshwater into the Bay of Bengal. Similarly, the southeast Asian rivers (Mikong and Siam, etc.) debauch enormous fresh water into the Indonesian Sea during the SW monsoon. Besides, a regional negative evaporation (minus) precipitation balance (–ve E–P) exists over the northeastern Indian Ocean and the Indonesian Sea[2]. Consequently, the surface salinity of the northeastern Indian Ocean and the Indonesian Sea is considerably lower (< 34.5 ppt) than the oceanic mean (35 ppt). In the western Indian Ocean, however, water remains highly saline (> 34.5 ppt) toward the Arabian Sea which does not receive major freshwater flux (except Indus, Narmada and Tapti rivers) besides having a positive regional evaporation (minus) precipitation (+ve E–P) budget[2]. These two extreme salinity watermasses are separated by an oblique boundary along 34.5 ppt isohaline (Figure 1 A) south of Sri Lanka[3]. The isohalines become sub-parallel in areas

south of 10°S latitude, representing a hydrographic front that separates northern monsoonal gyre from southern subtropical gyre[3]. Wyrtki[4] described it as the 10°S hydrographic front, a major oceanographic boundary characterized by unique salinity, temperature, oxygen contents from the surface waters to the abyssal depth extending from south of Java to Madagascar. The area is
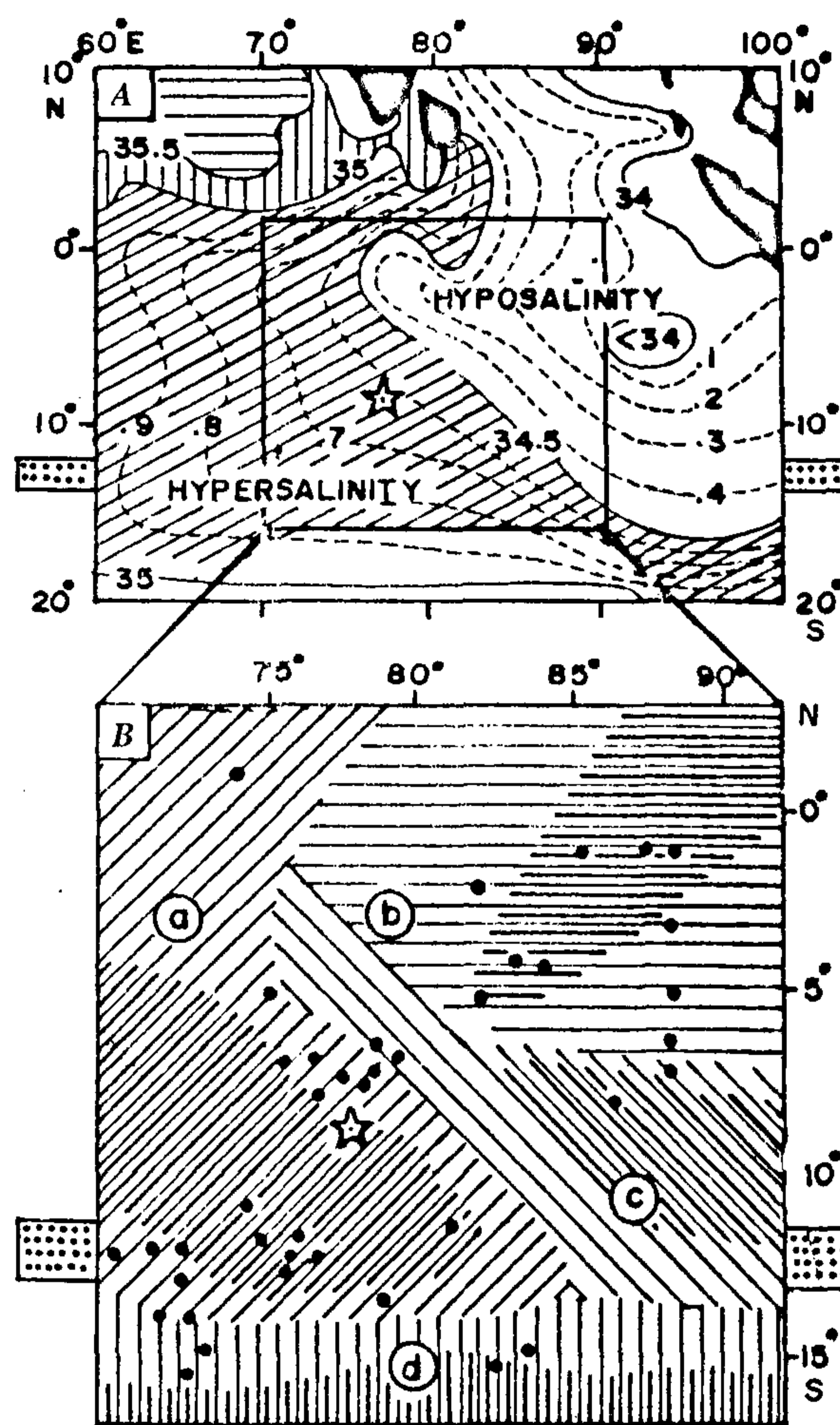
Figure 1. Modern surface salinity during July–August and related radiolarian factors in the central tropical Indian ocean. A, Surface salinity during July–August[3] divides the central Indian Ocean obliquely along the 34.5 ppt isohaline into SW hypersaline (>34.5 ppt) and northeastern hyposaline (<34.5 ppt) parts. B, Locations of 42 Holocene surface sediments (dots) and four radiolarian factors in the central Indian Basin. Double and single lines depict >0.7 and >0.5 factor loadings respectively. a, SW hypersaline factor 1; b, Northeast hyposaline factor 2; c, Transitional boundary-line factor 3 along 34.5 ppt isohaline south of Sri Lanka[3]; d, Southern factor 4 representing Wyrtki's[4] hydrographic front at 10°S. Asterisk mark is the location of sediment core SK-69/1.

Table 1. Sample numbers, latitudes, longitudes, water depth of 42 surface sediments and their respective communalities and factor loading matrix after varimax rotation

Sample no.	Latitude	Longitude	Water depth	Communality	Factors (assemblages)			
					Southwest (F1)	Northeast (F2)	Transitional (F3)	Southern (F4)
RVG 2483	02.050 S	82.079 E	4590 m	0.86144	−0.47741	−0.65004	−0.44852	0.09898
RVG 2486	05.000 S	82.090 E	4990 m	0.87629	−0.38617	−0.70803	−0.40199	0.25349
RVG 2494	04.000 S	83.190 E	3750 m	0.86572	−0.24726	−0.53067	−0.63079	0.35367
RVG 2501	04.000 S	84.000 E	4860 m	0.89063	−0.29106	−0.82378	−0.16679	0.31539
RVG 2513	01.080 S	85.000 E	4600 m	0.91146	−0.32587	−0.78788	−0.27978	0.32595
RVG 2520	01.125 S	87.020 E	4600 m	0.87957	−0.22177	−0.78658	−0.41872	0.19065
RVG 2528	08.070 S	86.109 E	5200 M	0.89504	−0.26691	−0.27413	−0.82478	0.26151
RVG 2531	07.012 S	88.155 E	5080 m	0.86860	−0.26158	−0.53161	−0.70482	0.14417
RVG 2532	06.001 S	88.090 E	5150 m	0.87537	−0.32955	−0.36418	−0.39331	0.69241
RVG 2533	05.075 S	88.180 E	5030 m	0.83807	−0.34545	−0.60744	−0.43951	0.39571
RVG 2535	03.062 S	88.065 E	4820 m	0.91742	−0.38536	−0.33708	−0.69327	0.41794
RVG 2237	01.059 S	88.095 E	4620 m	0.91334	−0.32799	−0.73511	−0.44973	0.25123
F 47	13.800 S	73.999 E	5150 m	0.93683	−0.72173	−0.33927	−0.47777	0.26939
F 56	14.002 S	73.001 E	4389 m	0.68780	−0.61231	−0.31733	−0.26013	0.38014
F 81	12.490 S	78.011 E	4977 m	0.88063	−0.66523	−0.23442	−0.57234	0.23573
F 99	05.000 S	75.992 E	4492 m	0.79227	−0.43174	−0.67206	−0.20912	0.33240
F 101	07.027 S	76.002 E	5290 m	0.85812	−0.74139	−0.35082	−0.20303	0.37970
F 150	07.644 S	78.954 E	4700 m	0.92248	−0.61965	−0.41068	−0.41431	0.44520
F 151	07.489 S	78.014 E	4750 m	0.90265	−0.53312	−0.52796	−0.48894	0.31722
F 152	07.840 S	77.980 E	NA	0.94388	−0.52815	−0.42385	−0.67137	0.18589
F 153	08.024 S	76.967 E	5000 m	0.92272	−0.77829	−0.20063	−0.51487	0.10794
F 154	07.067 S	76.989 E	NA	0.92586	−0.60898	−0.60671	−0.20632	0.37991
F 155	07.004 S	78.495 E	NA	0.88516	−0.61375	−0.37346	−0.55338	0.25053
F 156	07.067 S	79.500 E	NA	0.87597	−0.61855	−0.26188	−0.53825	0.36754
F 157	06.868 S	77.669 E	NA	0.91415	−0.59119	−0.50440	−0.45089	0.32699
F 158	06.506 S	78.945 E	NA	0.86084	−0.48506	−0.59623	−0.41634	0.31100
F 199	12.337 S	76.377 E	5400 m	0.90312	−0.53190	−0.21895	−0.66120	0.36753
F 379	01.089 N	74.670 E	2475 m	0.80524	−0.45336	−0.38856	−0.47925	0.46803
SS 105	11.010 S	74.985 E	5022 m	0.93133	−0.69447	−0.36103	−0.48079	0.29587
SS 120	13.006 S	72.984 E	4300 m	0.95222	−0.69579	−0.32206	−0.50242	0.33458
SS 121	12.007 S	73.073 E	4430 m	0.91740	−0.69414	−0.51251	−0.37659	0.17630
SS 124	12.017 S	73.000 E	4390 m	0.92241	−0.48775	−0.38600	−0.59912	0.42020
SS 126	14.019 S	72.016 E	4310 m	0.92419	−0.42492	−0.55081	−0.21443	0.62790
SS 127	11.999 S	70.990 E	4750 m	0.92951	−0.59395	−0.50013	−0.42112	0.38635
SS 128	11.969 S	75.465 E	5007 m	0.94471	−0.60484	−0.33927	−0.60922	0.30435
SS 129	12.006 S	76.452 E	5100 m	0.91840	−0.75998	−0.37402	−0.23737	0.38025
SS 139	11.514 S	81.490 E	5085 m	0.94777	−0.70351	−0.39004	−0.33471	0.43436
SS 183	13.510 S	78.979 E	5388 m	0.91224	−0.47417	−0.37737	−0.34235	0.65406
SS 206	15.090 S	83.560 E	NA	0.94385	−0.54120	−0.34848	−0.54670	0.48025
SS 210	15.487 S	82.950 E	5040 m	0.75740	−0.29804	−0.30430	−0.23992	0.72001
SS 231	14.890 S	73.530 E	4900 m	0.91914	−0.51804	−0.36101	−0.47454	0.54338
SS 241	15.500 S	72.991 E	4650 m	0.91468	−0.68373	−0.45363	−0.14932	0.46809
				Percentage of variance	28.89	23.41	21.99	14.86
				Cumulative variance	28.89	52.89	74.29	89.16

influenced by the south equatorial current which has seasonal fluctuations, i.e. minimal during NE monsoon $(40 \times 10^6 \text{ m}^3/\text{s})$ and maximum during SW monsoon $(54 \times 10^6 \text{ m}^3/\text{s})$. It transports low salinity water off northwest Australia due to the Indo-Pacific through flow (IPT)[3-4].

Because majority of living radiolaria inhabit the top 100 m of oceanic watermass[5], the International Indian Ocean Expedition (IIOE) hydrographic vertical profiles[3] in the study area from 0 to 300 m watermass suggested that the radiolaria may record changes in surface salin-

ity, temperature and productivity of top ~100 m waters[6]. In the present paper, we have refined radiolarian factor assemblage model of Gupta[7] by relinquishing the rare groups (<2% abundance) that caused noise and suppressed the environmental signals. Percentage data of radiolarian groups[6-8] from the Holocene surface sediments[6-7] were statistically analysed to relate the faunal assemblages with the monsoonal sea-surface salinity (SSS), temperature (SST) and potential primary productivity (PPP). Later, we quantified down-core faunal assemblages to ascertain paleomonsoonal changes in a

Table 2. Correlation matrix between 4 modern radiolarian factors from the Holocene samples and the modern sea surface salinity, productivity and temperature[3,13]

	Factor-1	Factor-2	Factor-3	Factor-4	Sal-NEM	Sal-fall	Sal-SW	Sal-Spr	PPP-NE	PPP-SW	SST-Dec	SST-Fall	SST-Aug	SST-spr
Factor-1	1.0000													
Factor-2	-0.5234	1.0000												
Factor-3	-0.1587	-0.3662	1.0000											
Factor-4	0.1232	0.2330	0.3621	1.0000										
Sal-NEM	-0.4754	0.4955	0.0899	0.2006	1.0000									
Sal-fall	-0.1101	-0.0770	0.2459	0.1240	0.4293	1.0000								
Sal-J-A	-0.7223	0.5170	0.2145	0.2439	0.6601	0.3726	1.0000							
Sal-Spr	0.5621	-0.3566	0.1881	0.3582	-0.1700	0.3321	-0.2698	1.0000						
PPP-NEM	0.0906	-0.2315	0.0203	-0.2060	0.0362	-0.1400	-0.0511	-0.0761	1.0000					
PPP-SWM	-0.7902	0.3157	0.1806	-0.0782	0.3456	0.1626	0.7727	-0.6476	-0.0340	1.0000				
SST-Dec	-0.0448	0.2761	-0.1476	0.0372	0.0576	-0.5499	-0.0074	-0.2586	-0.0024	-0.0346	1.0000			
SST-Fall	0.3042	-0.2260	-0.2417	-0.3244	-0.4406	-0.7487	-0.5518	-0.1213	0.5301	-0.3805	0.3387	1.0000		
SST-Aug	0.5036	-0.4824	-0.0929	-0.3293	-0.4965	-0.3537	-0.6692	0.1844	0.5840	-0.5173	-0.0064	0.8113	1.0000	
SST-spr	0.4060	-0.5513	-0.2646	-0.6339	-0.4772	-0.1201	-0.6707	0.0422	0.3026	-0.3959	-0.1094	0.5111	0.6607	1.0000

Note: Values > 0.489, 0.393, 0.357, 0.304 and 0.257 are significant at 0.001 (99.9%), 0.001 (99%), 0.02 (98%), 0.05 (95%) and 0.1 (90%) levels respectively. Spring = May, June and July, Fall = Nov, Dec. and Jan (Levitus[13]).
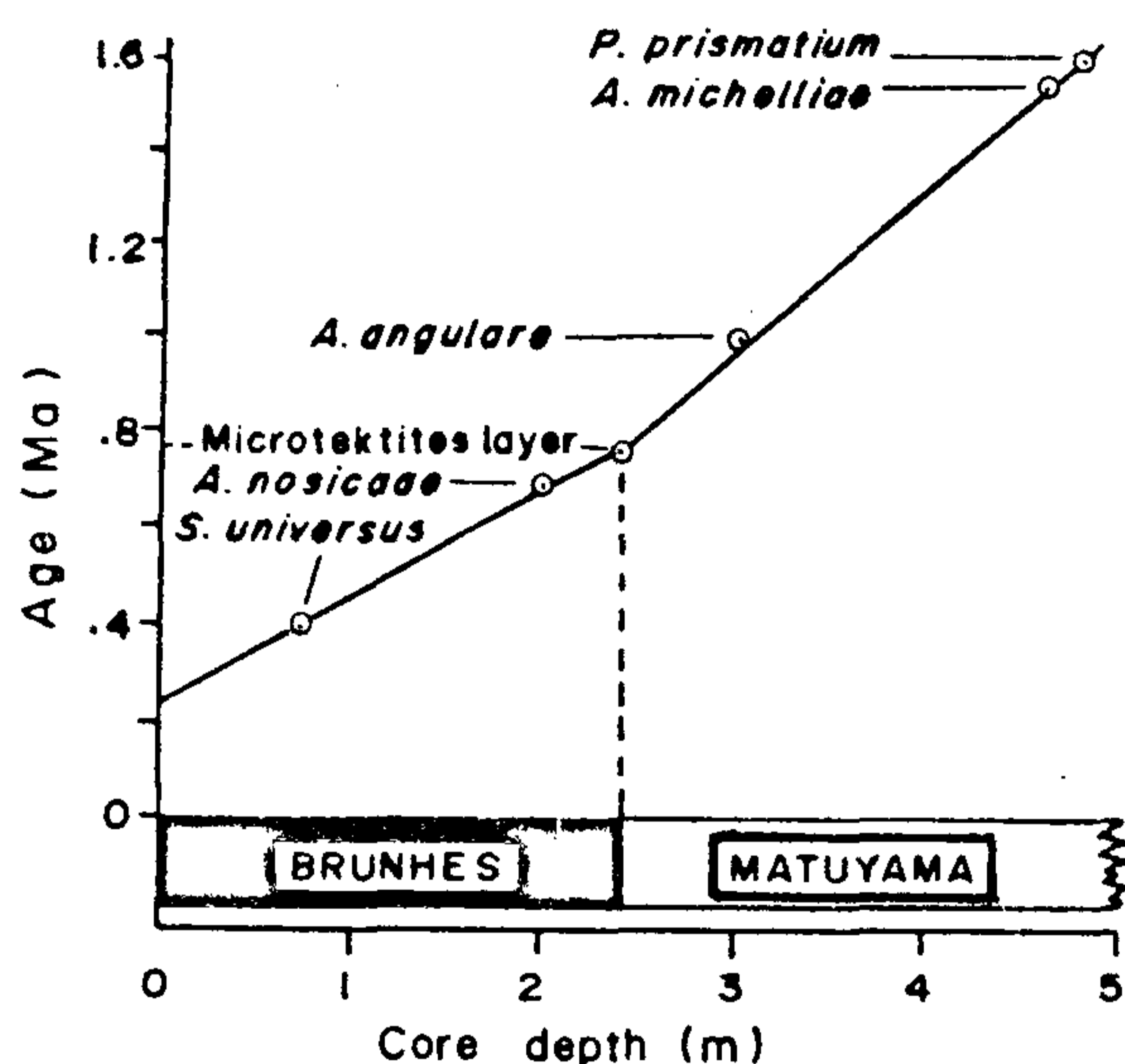

Figure 2. Stratigraphic control of SK-69/1 core bracketed by radiolarian extinction levels[9,17] and Australasian microtektite maxima[14] near Brunhes/Matuyama boundary[15,16]. The first 200 ka record was not recovered.
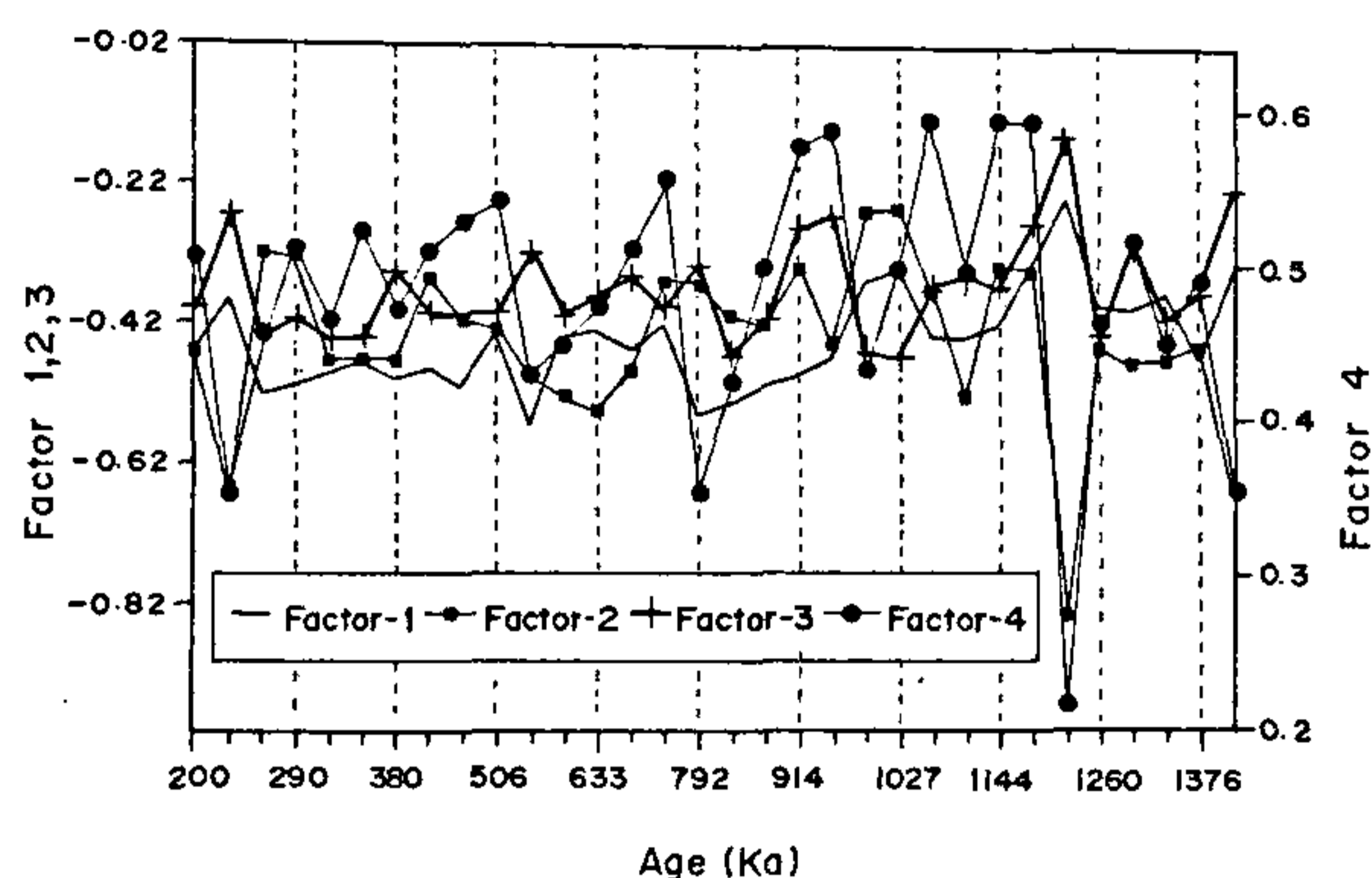

Figure 3. Down-core fluctuation in the radiolarian paleofactors in a Quaternary sediment core SK-69/1. Paleofactors, 1, 2 and 3 oscillated within -0.72 to -0.15, whereas factor 4 oscillated within 0.2 to 0.6 factor values at the core site in the last 200–1400 ka. Approximately 10-peaks (in 1.2 Myrs) of factor-4 suggested oscillation of Wyrtki's[4] 10°S hydrographic front due to changes in monsoonal freshwater flux apparently at 120,000 yrs (± 20,000) cycle in the Quaternary tropical Indian ocean.

sediment core (SK-69/1), which has an excellent geological record for the last ~200,000–1,400,000 years (Quaternary) in the central tropical Indian Ocean.

Based on the sedimentation rate of ~1 cm/1000 years [1000 years = kiloyears (ka)] for the top sections of VM-34-53 (0–236 cm = 210 ka) and RC-14-22 (0–100 cm = 120 ka) sediment cores[9], the 42 surface sediments (top 2–3 cm of the sea floor) from the central Indian Basin represented the Holocene material (Figure 1 B). Gupta[6,7] quantified 47 radiolarian groups[8] from these Holocene samples following the random settling method of Moore[10]. Out of the forty-seven, 22 groups contributed <2% abundance and added to the random

noise in earlier analysis[7]. In the present analysis, 25 groups qualified the standard criteria of Imbrie and Kipp[11], i.e. (i) relinquishing of groups contributing <2% which only cause the noise, (ii) surface water dwellers and (iii) modern analogues of the fossil groups. Percentage data of 25 groups were analysed by Imbrie and Kipp's[11] method for Q-mode factors, which resolved four varimax factors accounting for 89.15% of distributional variance (v) explained (Table 1). Communality value ($h^2 > 0.89$), which is the internal check for the distortion of data due to differential dissolution, taxonomic inadequacy or the local ecological anomalies, is sufficiently higher than the Imbrie et al.'s[12] threshold (0.8) for the meaningful interpretations. The first factor ($v = 28.88\%$, dominant groups Artiscin and Pyloniids) with highest loading in the southwestern area [Figure

1 B(a)] is related with hypersaline (> 34.5 ppt) water-mass (Figure 1 A). The second factor (v = 23.41%, dominant groups *Spongaster.* and Spongodiscids) with highest loading in the northeastern area [Figure 1 B(b)] is related to low salinity (<34.5 ppt) watermass (Figure 1 A). The third factor (v = 21.98%, dominant groups *Disolenia* and *Collosphaera*) is a transitional assemblage [Figure 1 B(c)] characterizing boundary-line salinity condition along the oblique 34.5 ppt isohaline south of Sri Lanka (Figure 1 A). The fourth factor (v = 14.86%, dominant groups *Lamprocyclas* and *Anthocyrtidium*) exhibited highest loading [Figure 1 B(d)] south of 10N°–12° S low salinity hydrographic front of Wyrtki[4]. The factor loading values were computed for correlation (Table 2) with modern surface salinity, SST and productivity by digitizing oceanographic charts of Wyrtki[3] and the seasonal oceanographic digital data of Levitus[13] on magnetic tapes at respective sampling locations. All factors are correlated well only with the SW monsoonal salinity, SST and PPP of the tropical Indian Ocean (Table 2) and concur with earlier study[7]. Results suggested that these factors, when studied in down-core, may provide insight into paleomonsoonal salinity, SST and PPP changes in the geological past.

Therefore, the down-core radiolarian factors (faunal assemblages) were studied in a sediment core SK-69/1 (Lat. 8.55°S, Long. 77°E, water depth 5388 m, Figure 1 B) to decipher monsoonal changes in the geological past. Recently, Shyamprasad and Sudhakar[14] encountered an Australasian microtektite (the melt-splash out fall after the collision of a meteorite on the Earth) maximum at 235 cm core-depth of SK-69/1. Earlier, Schneider et al.[15] reported such microtektite maximum to occur at around the Brunhes–Matuyama (B/M) geomagnetic reversal boundary, which is isotopically dated by Baksi et al.[16] at ~780 ka before present. Other stratigraphic controls of the sediment core are based on the identification of the extinction levels of *Stylatractus universus* (425 ka)[17], *Anthocyrtidium nosicaae* (700 ka), *Anthocyrtidium angulare* (1000 ka), *Anthocyrtidium michellinae* (1500 ka) and *Pterocanium prismatium* (1600 ka)[9] in the core (Figure 2). Based on these datum levels, the sedimentation rates of Brunhes and Matuyama periods were calculated by plotting datum level vs core depth (Figure 2). As the sedimentation rates of the Brunhes (4.2 mm/ka) and Matuyama (2.8 mm/ka) have a ratio of 3:2, we selected subsamples at 15 cm and 10 cm intervals respectively to maintain regular age-spacing [delta-t ~39.5-ka ± 8-ka] in down-core data on radiolarian faunal assemblages. The percentage data on down-core radiolarian fauna were analysed for Q-mode factors by the same method used for the Holocene samples in the present study. Fluctuations in the down-core factor values (paleo-factors) suggested paleomonsoonal changes in salinity, SST and PPP with respect to core depth (Figure 3) as per their relationship

in the Table 2. However, troughs of the factor-4 indicated higher freshwater flux during warmer periods, resulting in southward migration of 10°S hydrographic front. Whereas, peaks of the factor-4 suggested less freshwater flux during colder periods, resulting in northward migration of 10°S hydrographic front in geological past. The results suggested that the 10°S hydrographic front has oscillated back and forth almost 10 times (10 peaks of factor 4, Figure 3) from its present position in 1.2 million years, suggesting an apparent cyclicity of ~120 ka (± 20 ka). Such ~100 ka cycle is a prominent feature in excellently preserved geological records[18-20], and it corresponds to the Earth's orbital eccentricity cycle[21]. Therefore, the 120 ka cycle apparently present in the oscillation of the 10°S hydrographic front is due to changes in the surface salinity at the core site. Recently, from the same core data-set, the paleo-sea surface temperatures reconstructed by the radiolarian transfer functions are also reported to oscillate cyclically at ~100 ka, corresponding to the Earth's orbital eccentricity cycles[22].

Obviously our core data have recorded the changes in the surface salinity over the core site (Figures 1 and 3) in the last 1.4 million years. These changes are possible by two mechanisms, i.e. (i) the regional precipitation over the central Indian Ocean coupled with monsoonal freshwater debauched by the Indian rivers into the Bay of Bengal; and (ii) the low salinity surface (0–100 m) and deep (>100–800 m) waters from the Indo-Pacific through flow (IPT) via deeper inner-ocean passages (depth range 70–1000 m) near Bali, Lombok, Savu and Timor Islands[23]. We analysed both possibilities to evaluate the sources of low salinity at core site. Figure 4 a depicts the rainfall over the Indo-Pacific region during July based on GOES precipitation index[24]. The oblique precipitation contours over the central Indian Ocean (Figure 4 a) are in conformation with the oblique 34.5 ppt isohaline shown in Figure 1 a, suggesting the salinity lowering at core-site is the consequence of the regional oceanic monsoonal precipitation coupled with the freshwater debauched into the Bay of Bengal by the Indian rivers. The mechanism of second possibility of IPT is related to the monsoonal winds, pressure gradient and surface currents in the Indo-Pacific region[25]. Surface water flows from the Java Sea and Pacific Ocean into the Banda Sea, causing an accumulation of warm low salinity water and a depressed thermocline due to unfavourable winds which are unable to move it into the Indian Ocean during NE monsoon. During SW monsoon strong southeast winds blow over the region, forming south equatorial current in the Indian Ocean between Java and Australia, generating strong southward flow of upper 200 m water towards Indian Ocean[25]. Because low salinity IPT surface water gushes towards Indian Ocean due to south-east winds, pressure gradient and the formation of south
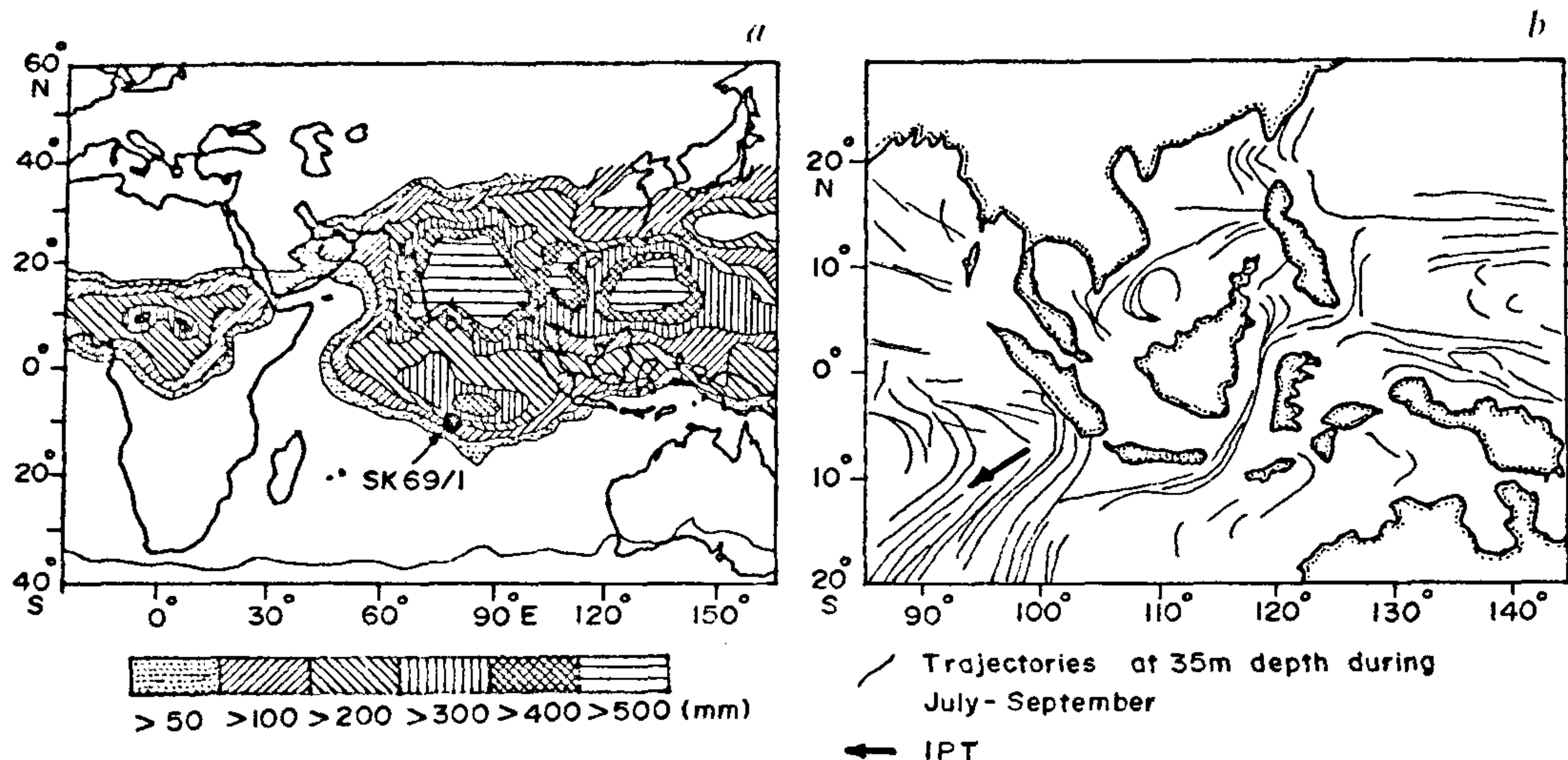
Figure 4. Possible sources of the freshwater causing low salinity at core site. *a*, The precipitation over the Indo-Pacific region showing that the core site is well within 200 mm rainfall during July[24]; *b*, The trajectories of the tracer particles released at 35 m water[23] to trace the Indo-Pacific through flow during SW monsoon showing that SW flowing IPT surface water affected areas beyond 15°S.

equatorial current, the possibility remains that some amount of IPT water might be reaching up to the core site. The trajectories of tracer particles, released at 35 m during different seasons, indicated that the IPT is very seasonal. During SW monsoon the trajectories are in SW direction (Figure 4 *b*) influencing the areas further south than the 10°S (Miyama et al.[23], Figures 11 *a–d*, Figures 18 *a, b*). Therefore, we surmised that surface IPT water has not much influence on the surface water-mass overlying our core site.

However, the possibility of IPT water advected from the sub-surface layers is not ruled out. Therefore, we summarized the vertical salinity profiles of the IIOE[3] during SW monsoon along the east–west transect at the equator, and north–south transects at 70°, 77°, 92° and 110°E longitudes from 0 to 15°S latitudes (Figure 5, index map). The vertical salinity structure (VSS) along equator from 70 to 87°E suggested that low salinity surface water (<100 m) floats over high salinity deep water (> 100 m) during SW monsoon (Figure 5 *a*). The VSS along 70°E from 0 to 17°S opined a low-salinity surface water (<34.8 ppt) down south up to 12°S, and a protrusion of low-salinity deep water of IPT origin below ~400 m (stippled, Figure 5 *b*). The VSS along 77°E from 5°N to 12°S showed low-salinity surface water (<100 m) and a deep low-salinity water of IPT origin (stippled) below 400 m (Figure 5 *c*). The VSS along 92°E indicated a low-salinity surface water (<100 m) and the intrusion of low-salinity deep water of IPT origin (from depth >700 to >100 m beneath the 10°S, Fig-

ure 5 *d*). The columnar advection of the low-salinity water of IPT origin (salinity 34.8 ppt, Fine[26], Table 1) represents the 10°S hydrographic front influenced by the IPT. The advection of low-salinity IPT from the deep is more pronounced in the eastern profile along 110°E from 10° to 25°S (Figure 5 *e*), which shows that low-salinity IPT water is almost inseparable from the surface low-salinity water (<100 m). The deeper low-salinity IPT water (<34.8 ppt) is easily recognizable from surface low-salinity watermass due to the regional precipitation coupled with freshwater flux into the Bay of Bengal towards west of 90°E (Figures 5 *b, c*). It becomes inseparable from the surface low-salinity water towards east (Figures 5 *d, e*). The surface low-salinity water of monsoonal origin (Figures 5 *b–d*) is distinctly due to the regional oceanic precipitation over the central Indian Ocean coupled with the freshwater flux from the Indian rivers into the Bay of Bengal, as it floats over the high-salinity subsurface water (> 100 m). This surface water is intruded by low-salinity deep water of IPT origin towards east of the 90°E (stippled columns, Figures 5 *b–e*). It suggested that fluctuations recorded by surface dwelling radiolarians (<100 m) in our core were not influenced by the intrusion of deep low-salinity IPT water at the core site.

In view of the above, the regional precipitation over the core site, the freshwater debauched by the Indian rivers into the Bay of Bengal and surface IPT occur during SW monsoon. These facts converge to our reasoning that the 100 ka cyclicity recorded in factor-4 is
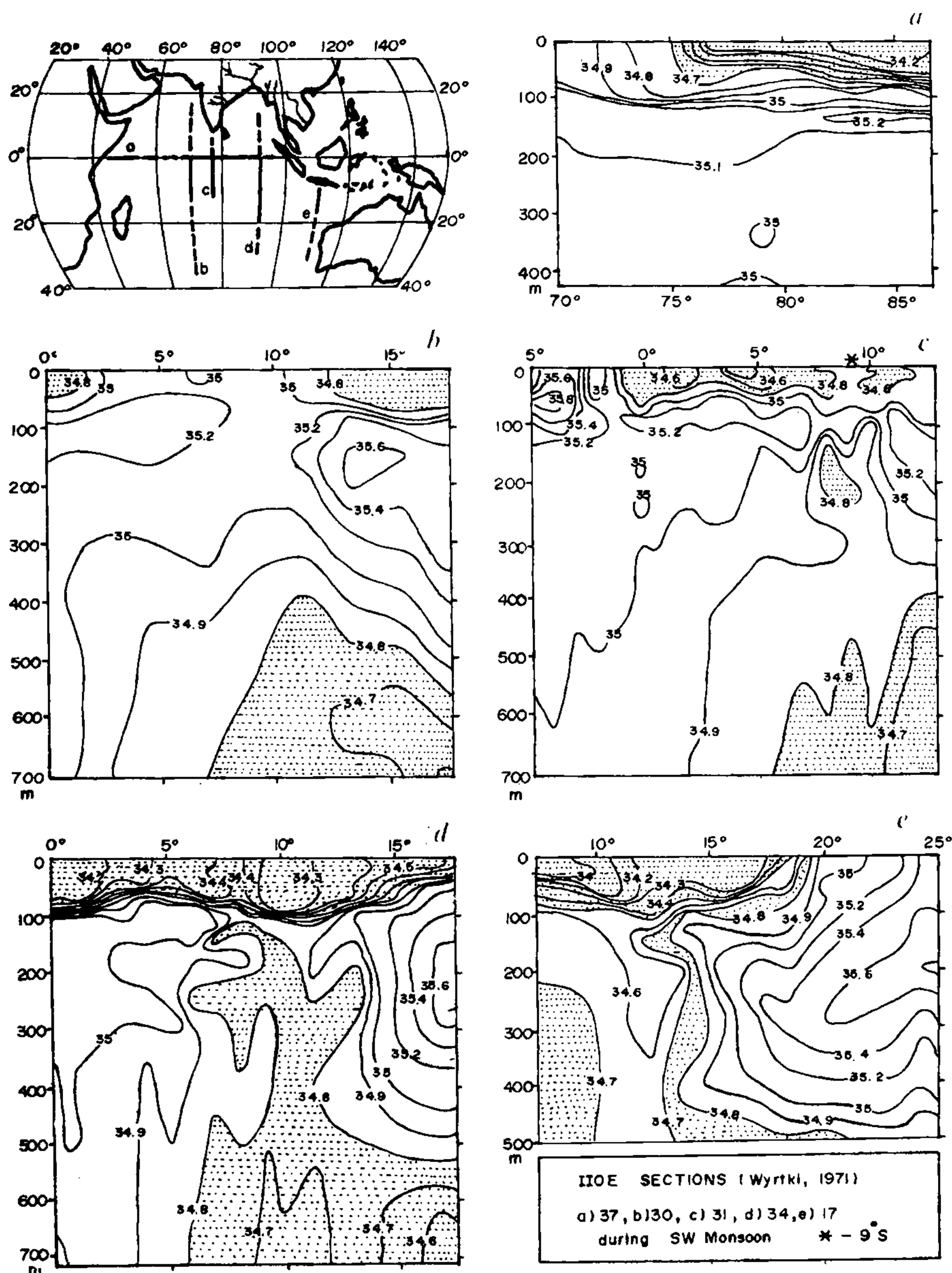
Figure 5. Vertical salinity structures in the equatorial Indian Ocean during SW monsoon. Index map showing the IIOE hydrographic profiles along the equator *a*, 70°E *b*, 77°E *c*, 92°E *d*, and 110°E *e* longitudes. Stippled area denotes low-salinity water masses at the surface (<100 m) due to monsoonal precipitation and deep advecting vertical columns of low salinity (> 400 m, 34.8 ppt[26]) representing the Indo-Pacific through flow[3].

related to the monsoonal fluctuation of the 10°S hydrographic front. The results suggested that radiolarian faunal assemblages in down-core exhibit the boundary-line monsoonal changes in surface salinity of the central Indian Ocean for the last 0.2–1.4 million years. The paleofactor values have potential for the reconstruction of

sea-surface salinity, using transfer function technique[11,22,27,28]. Our ~0.2–1.4 million years monsoonal record is larger than 350 ka paleomonsoonal record based on eolian dust flux from Arabian desert[29] to the Indian Ocean. Though results suggested that 10°S hydrographic front has oscillated due to monsoon with

~120 ka eccentricity cycle, its verification requires a high-resolution study because strength of monsoon is strongly affected by the precession (23 ka) and obliquity (41 ka) cycles[30] than the eccentricity cycle (100 ka, range ~95–135 ka). Our results of ~120 ka orbital eccentricity cycles related monsoonal oscillation in the 10°S hydrographic front open an unorthodox view that even though the amplitude of insolation related to the orbital, eccentricity cycles (~100 ka) may be low <0.1%), compared to precession (23 ka) and the obliquity (41 ka) cycles[31], its modulating effect on the Asian monsoon system cannot be denied and ignored.

1. Carroll, J., Falker, K. F., Brown, E. T. and Moore, W. S., *Geochim. Cosmochim. Acta*, 1993, 57, 2981–2990.
2. Oberhuber, J. M., Max Plank Institut fur Metereologie Report, 1988, p. 15.
3. Wyrtki, K., *The Oceanographic Atlas of the International Indian Ocean Expedition*, NSF, Washington DC, 1971, p. 531.
4. Wyrtki, K., in *The Biology of the Indian Ocean* (ed. Zietschel, B.), Springer-Verlag, New York, 1973, pp. 18–36.
5. Dworetzky, B. A. and Morley, J. J., *Mar. Micropaleontol.*, 1987, 12, 1–19.
6. Gupta, S. M., Ph D thesis, Goa University, 1991, p. 338.
7. Gupta, S. M., *J. Geol. Soc. India*, 1996, 47, 339–354.
8. Gupta, S. M. and Srinivasan, M. S., *Micropaleontology*, 1992, 38, 209–236.
9. Johnson, D. A., Schneider, D. A., Nigrini, C. A., Caulet, J. P. and Kent, D. V., *Mar. Micropaleontol.*, 1989, 14, 33–66.
10. Moore, T. C., *J. Sediment. Petrol.*, 1973, 43, 904–906.
11. Imbrie, J. and Kipp, N. G., in *The Late Cenozoic Glacial Ages* (ed Turekian, K. K.), Yale Univ., New Haven, Conn., 1971, pp. 71–181.
12. Imbrie, J., Donk, J. V. and Kipp, N. G., *Quat. Res.*, 1973, 3, 10–38.
13. Levitus, S., *Climatic Atlas of the World Ocean*, Washington DC, 1982, pp. 173.
14. Shyamprasad, M. and Sudhakar, M., *Meteoritics Planet. Sci.*, 1996, 31, 46–49.
15. Schneider, D. A., Kent, D. V. and Mellow, G. A., *Earth Planet. Sci. Lett.*, 1992, 111, 395–405.
16. Baksi, A. K., Hsu, V. McWilliams, M. O. and Farrar, E., *Science*, 1992, 256, 356–357.
17. Hays, J. D. and Shackelton, N. J., *Geology*, 1976, 4, 649–652.
18. Crowley, T. J., Kim, K-Y., Mengel, J. G. and Short, D. A., *Science*, 1992, 255, 705–707.
19. Hays, J. D., Imbrie, J. and Shackelton, N. J., *Science*, 1976, 194, 1121–1132.
20. Imbrie, J. et al., *Paleoceanography*, 1993, 8, 699–735.
21. Berger, A. L. and Loutre, M. F., *Quat. Sci. Rev.*, 1991, 10, 297–317.
22. Gupta, S. M., Fernandes, A. A. and Mohan, R., *Geophys. Res. Lett.*, 1996, 23, 3159–3162.
23. Miyama, T., Awaji, T., Akitomo, K. and Imasato, N., *J. Geophys. Res.*, 1995, 100, C10, 20517–20541.
24. *Climate Diagnostic Bull.*, 1995, 95, T24.
25. Wyrtki, K., *J. Geophys. Res.*, 1987, 92, C12, 12941–12946.
26. Fine, R. A., *Nature*, 1985, 315, 478–480.
27. Wang, L., Sarnethein, M., Duplessy, J. C., Erlenkeuser, H. and Jung, S., *Paleoceanography*, 1995, 10, 749–761.
28. Gupta, S. M. and Fernandes, A. A., *Bull. Indian Geologists Assoc.*, 1995, 18, 29–51.
29. Shinmield, G. B., Mowbray, S. R. and Weeden, G. P., *Trans. R. Soc. Edinburgh. Earth Sci.*, 1992, 81, 289–299.
30. Clemens, S. C., Murray, D. W. and Prell, W. R., *Nature*, 1996, 274, 943–948.
31. Clemens, S. C. and Tiedemann, R., *Nature*, 1997, 385, 301–304.

Occurrence of Fe, Mn-rich layer in the distal Bengal fan

S. V. S. Pavana Putra, M. Lucy Gray, P. B. Murty and A. S. R. Swamy

Department of Geology, Andhra University, Visakhapatnam 530 003, India

Dark tan-coloured Fe, Mn-rich stiff layer was observed at 45–50 cm and 40–42 cm levels in the Sagar Kanya 72/1 and 100/6 sediment cores respectively, which were collected from distal Bengal fan under BOBCRUST programme. SK 72/1 and SK 100/6 cores were analysed for Fe, Mn, Ni, Co, Cr, $CaCO_3$ and organic carbon (OC) contents. A remarkable increase in Fe, Mn and drastic decrease in $CaCO_3$, OC, compared to overlying and underlying sediment layers was observed at this stiff layer. Change of these elements concentration correlates with the change of fauna from the cold assemblage to warm assemblage. Increase of Fe, Mn, Ni, Co and decrease of Cr, $CaCO_3$, OC indicate that this layer is formed due to post-depositional migration of these elements during the Pleistocene/Holocene transitional period, because of emasculated influence of terrestrial input into these sites.

BENGAL fan is the world's largest submarine fan, which is positioned under the highest run-off receiving bay, and it is built of terrigenous sediments carried from the Himalayan region by the Ganges, Brahmaputra, Irrawaddy and Salween river systems[1,2]. Variations in the run-off are dependent on the monsoons and the waning and waxing of glaciers in the catchment region. The sediment input is mainly controlled by a number of factors such as turbidity currents, sediment flow or fluvial input to the sea, giving rise to these thick fan sediments. Geochemical character of the sediment column reveals such variations and helps in identifying metal sources apart from providing a clue to their removal mechanism from the overlying water column[3,4]. Studies on Bengal fan deep sea cores are very few[5-10], published geochemical